Available online at www.sciencedirect.com
SciVerse ScienceDirect
Ceramics International 38 (2012) 3763–3771
CERAMICS INTERNATIONAL
www.elsevier.com/locate/ceramint

The effect of precipitant concentration on the formation procedure of yttrium aluminum garnet (YAG) phase

Liang Wang [a,b], Huamin Kou [a], Yanping Zeng [a], Jiang Li [a], Yubai Pan [a,*], Xingwei Sun [a], Jingkun Guo [c]

[a] Key Laboratory of Transparent and Opto-functional Inorganic materials, Shanghai Institute of Ceramics, Chinese Academy of Sciences, 1295 Ding Xi Road, Shanghai 200050, PR China
[b] Graduate School of the Chinese Academy of Sciences, 19A Yuquan Road, Beijing 100039, PR China
[c] State Key Laboratory of High Performance ceramics and Superfine Microstructures, Shanghai Institute of Ceramics, Chinese Academy of Sciences, 1295 Ding Xi Road, Shanghai 200050, PR China

Received 28 December 2011; received in revised form 6 January 2012; accepted 10 January 2012
Available online 16 January 2012

Abstract

In this paper, the effect of precipitant concentration on the formation procedure of YAG phase, which is actually a solid reaction controlled by the diffusion of aluminum ions into the yttria particles, is investigated. Under higher precipitant concentration, the size of yttria particles formed is in micron level and alumina particle is in the form of clusters of small particles. Therefore the element diffusion distance is lengthened and higher temperature ($\geq$1350 °C) is essential for the completion of phase transitions. Under lower precipitant concentration, the sizes of yttria particles and alumina particles are both smaller than 100 nm and two kinds of oxides are mixed uniformly, so the phase transition procedure can complete at lower temperatures ($\leq$1200 °C).

Keywords: Precipitation; Precipitant concentration; Phase transition; Yttrium aluminum garnet

1. Introduction

Yttrium aluminum garnet (YAG, $Y_3Al_5O_{12}$) exhibits cubic structure and the space group is *Ia*3*d*. Yttrium aluminum garnet ceramics with good optical properties can be prepared successfully because of no birefringence [1]. And besides, transparent YAG ceramics have good chemical stability and creep resistance [2,3]. Especially, when doped with rare earth elements, such as neodymium, ytterbium, cerium, YAG ceramic can be used as ideal solid-state laser materials and scintillating materials [4–6].

Nanopowder technology combined with vacuum sintering method is proved as an effective process for the fabrication of transparent YAG ceramics [7,8]. For the preparation of YAG nanopowder, precipitation method has attracted considerable attention because YAG powders with high sinterability can be prepared through this method. Many time and efforts have been put into the research on YAG powder synthesis using precipitation method. In previous works, transparent YAG ceramics have been tried to fabricate through precipitation method, and a certain amount of research focused on the process details have been conducted, for example, the type of precipitant [9], the reaction temperature [10], the introduction of dispersant [11], and the type of drying method [12]. But the effect of precipitating parameters on the formation procedure of YAG phase during calcining is seldom investigated. In order to get a comprehensive understanding of precipitation method for YAG powder preparation and to synthesize YAG powders with better sinterability, the research on the phase transition procedure and the effect of precipitating parameters on that procedure is necessary.

In this paper, YAG powders are prepared using coprecipitation method and mixed precipitation method, and the effect of precipitant concentration on the phase transition is investigated. The mechanism of concentration effect is explained from the viewpoint of ions diffusion.

---

* Corresponding author. Tel.: +86 21 52412820; fax: +86 21 52413903.
E-mail address: ybpan@mail.sic.ac.cn (Y. Pan).

0272-8842/$36.00 © 2012 Elsevier Ltd and Techna Group S.r.l. All rights reserved.
doi:10.1016/j.ceramint.2012.01.022

2. Experimental procedures

Yttrium nitrate hydrate ($Y(NO_3)_3{\cdot}6H_2O$, purity > 99.9%), aluminum nitrate hydrate ($Al(NO_3)_3{\cdot}9H_2O$, purity > 99.9%) and ammonium bicarbonate (NH_4HCO_3, analytical reagent) were used as raw materials. And the starting solutions were made by dissolving the corresponding raw materials into deionized water followed by filtering.

YAG precursors were prepared using two kinds of precipitation methods, reverse striking coprecipitation method and mixed precipitation method. The process flows of those two methods are shown in Fig. 1. As illustrated in Fig. 1, YAG was prepared by adding the metal ions solution which can give the garnet composition dropwise into ammonium bicarbonate solution under mild agitation for reverse striking coprecipitation process. While for mixed precipitation process, the aluminum ions were first precipitated using reverse striking precipitation method (the metal ions solution is added into the precipitant solution under mild agitation), then the aluminum precipitate was dispersed into the yttrium ions solution to form uniform suspension after being aged and washed using deionized water. After that, the yttrium ions in the suspension were precipitated using normal striking method (the precipitant solution is added into the metal ions solution under mild agitation) to obtain mixed precipitate, that is YAG precursor. YAG precursors obtained using different precipitation method were both washed using deionized water and alcohol and then dried and calcined at different temperatures for 2 h. The alumina precursor and yttria precursor were also prepared separately in order to investigate the effect of precipitant concentration on the formation procedure of YAG phase. The alumina precursor was prepared using reverse striking precipitation method under different precipitant concentrations. The yttria precursor was prepared using reverse striking precipitation method and normal striking precipitation method under different precipitant concentrations. The alumina and yttria precursors were calcined at 750 °C for 2 h. The experiment parameters referred in this paper are listed in Table 1. In Table 1, "C" and "M" are used to label precursors prepared using reverse striking coprecipitation method and mixed precipitation method, respectively, and "CC" and "MC" are used to label powders obtained by calcining corresponding precursors at 750 °C. In the same way, "A", "Y", "AC" and "YC" are used to label alumina and yttria precursors and calcined powders obtained at 750 °C.

Table 1
The experiment parameters referred in this paper.

	Precipitant concentration (mol/L)		Precipitation method	Powders obtained at 750 °C
	For Al^{3+}	For Y^{3+}		
C1	0.5		Coprecipitation	CC1
C2	1.5		Coprecipitation	CC2
M1	1.5	1.5	Mixed Precipitation	MC1
M2	1.5	0.5	Mixed Precipitation	MC2
M3	0.5	0.5	Mixed Precipitation	MC3
A1	0.5	–	Reverse Striking	AC1
A2	1.5	–	Reverse Striking	AC2
Y1	–	0.5	Normal Striking	YC1
Y2	–	1.5	Normal Striking	YC2
Y3	–	0.5	Reverse Striking	YC3

The phase analysis was performed using diffractometer (XRD, Model D/MAX-2550V, Rigaku, Tokyo, Japan) using Cu Kα radiation at the scanning speed of 10°/min (2θ). The morphologies of powders were observed using field emission scanning electron microscope (FESEM, Model JSM-6700F, JEOL, Tokyo, Japan).

3. Results and discussion

3.1. Phase transition procedure of YAG precursors

Fig. 2 shows the X-ray diffraction analysis of phase compositions of powders obtained at different temperatures by calcining precursors prepared through coprecipitation method under different precipitant concentrations. As shown in Fig. 2, the precipitant concentration has a great effect on the phase transition procedure of YAG precursors.

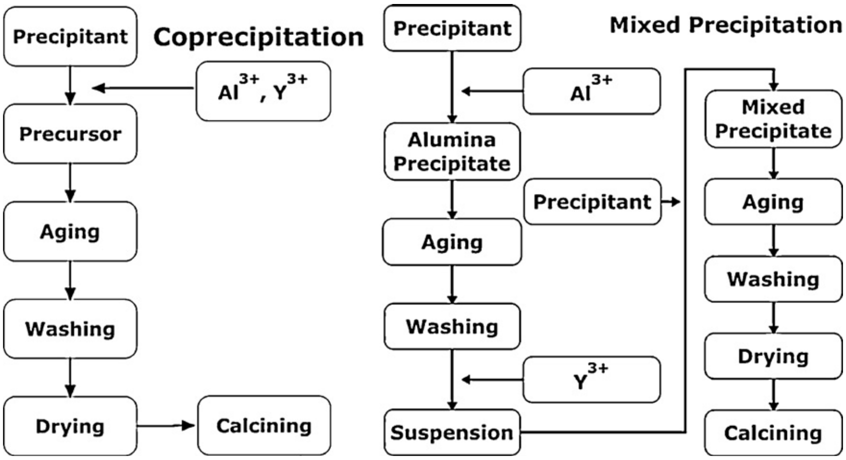

Fig. 1. The flow charts of coprecipitation method and mixed precipitation method.

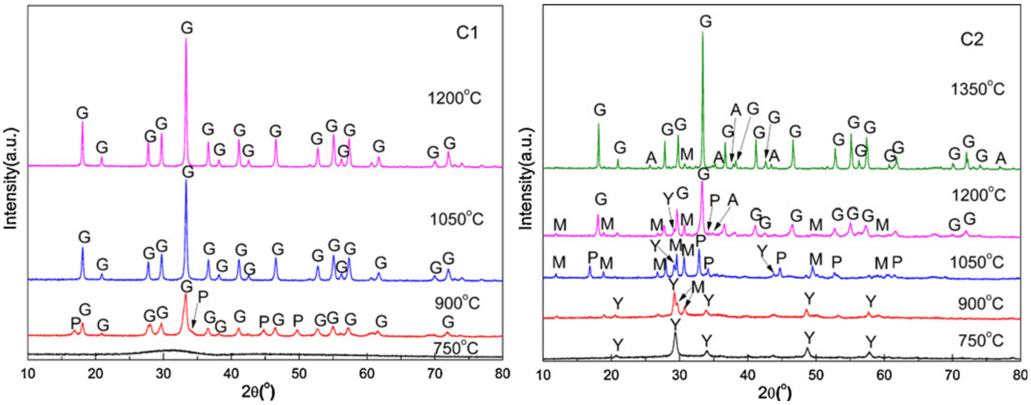

Fig. 2. The X-ray diffraction analysis of phase transition procedure of C1 and C2 (A: α-Al_2O_3, Y: Y_2O_3, M: YAM, P: YAP, G: YAG).

For precursor C1, the intermediate phase of yttrium aluminum monoclinic (YAM, $Y_4Al_2O_9$) is not detected clearly throughout the phase transformation process. The powder obtained at 900 °C consists of YAG phase and another intermediate phase yttrium aluminum perovskite (YAP, $YAlO_3$). When the temperature increases to 1050 °C, only diffraction peaks corresponding to YAG phase can be detected. With further increase of temperature, the only difference observed is the increase of the crystallinity of powder which can be certified by the increase in the relative intensity of diffraction peaks.

While for precursor C2, only cubic yttria phase can be detected in the powder obtained at 750 °C. When the temperature increases to 900 °C, YAM phase begins to appear, but cubic yttria phase is still the major phase in the powder obtained. Only YAM and YAP phases can be detected in the powder obtained at 1050 °C. The powder obtained at 1200 °C consists of YAG phase mainly with the minor phases of YAM, YAP, cubic yttria phase and α-Al_2O_3 phase coexisting. For the powder obtained at 1350 °C, YAG is the dominant phase, and YAP is not detected. YAM and alumina phases can still be detected although the corresponding peaks are quite weak even after the precursor being calcined at 1350 °C.

Fig. 3 shows the phase transition procedures of YAG precursors prepared through mixed precipitation method when changing the precipitant concentrations for precipitating aluminum and yttrium ions.

For precursor M1, the phase transition procedure is similar with the situation of C2. Only diffraction peaks corresponding to cubic yttria phase can be detected in the calcined powder obtained at 750 °C, and YAM phase begins to appear in the powder obtained at 900 °C. When the temperature increases to 1050 °C, the major phase in the powder obtained is YAM phase, and YAP phase begins to appear in this powder. And a certain amount of cubic yttria phase can still be detected. YAM, cubic yttria, YAG and YAP coexist in the calcined powder obtained at 1200 °C, and the strongest diffraction peak corresponds to the YAM phase. With further increase of temperature, the powder obtained at 1350 °C is composed of YAG, YAM and alumina phase, and the major phase is YAG.

For precursor M2, when it is calcined at 750 °C, no other phases can be detected except for cubic yttria phase. And the powder obtained at 900 °C is composed of YAM and YAP phases. When the calcining temperature increases to 1050 °C, only YAP phase can be detected. With further increase of temperature, only YAG phase can be detected in the calcined powder obtained at 1200 °C. When the temperature is further increased, the only difference observed is the increase of powder crystallinity which can be certified by the increase of diffraction peak intensity.

For precursor M3, when it is calcined at 750 °C, only cubic yttria phase can be detected. When the temperature increases to 900 °C, the powder is composed of YAM and YAP phases, which is quite similar with the situation of M2. But the situation of M3 at 1050 °C is quite different with M2. Only YAG phase can be detected in the powder obtained at this temperature. But the situation of M3 at 1050 °C is quite different with M2. Only YAG phase can be detected in the powder obtained at this temperature. With further increase of temperature, no obvious difference is observed.

The phase compositions of powders obtained by calcining precursors at different temperatures are summarized in Table 2. When multiphase coexisting occurs, the phases detected are

Table 2
The phase compositions of powders obtained at different temperatures for each experiment (A: α-Al_2O_3, Y: Y_2O_3, M: YAM, P: YAP, G: YAG).

	750 °C	900 °C	1050 °C	1200 °C	1350 °C
C1	–	P	G	G	–
C2	Y	Y, M	P, M, Y	G, M, Y, P, A	G, M, A
M1	Y	Y, M	M, Y, P	M, Y, G, P, A	G, M, A
M2	Y	M, P	P	G	G
M3	Y	M, P	G	G	–

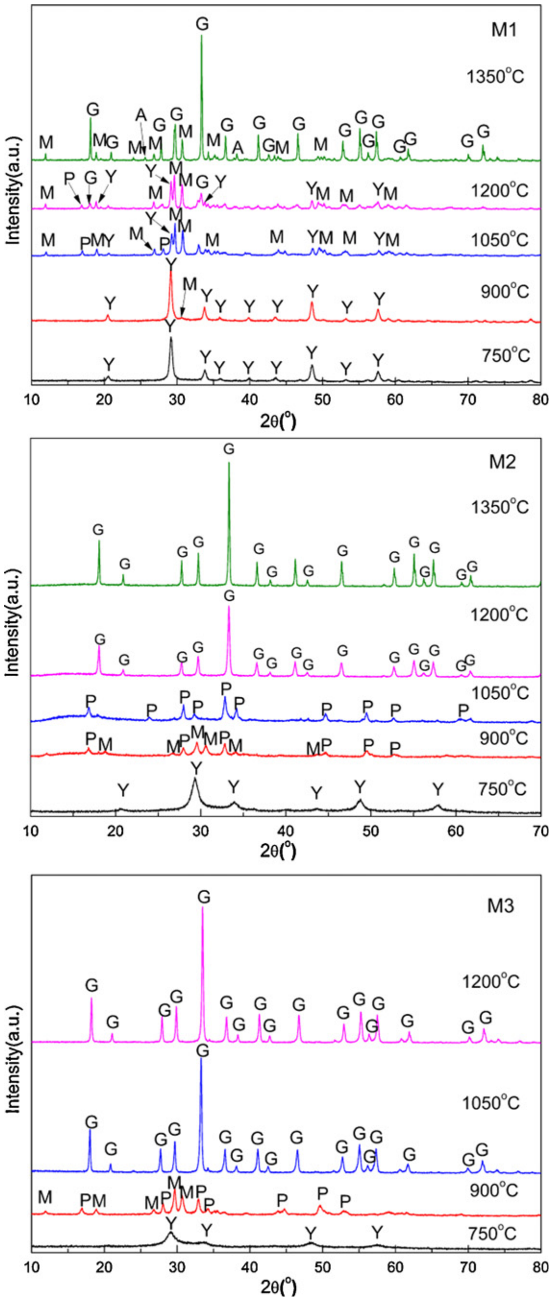

Fig. 3. The X-ray diffraction analysis of phase transition procedures for M1–M3 (A: α-Al_2O_3, Y: Y_2O_3, M: YAM, P: YAP, G: YAG).

ordered according to relative content which can be determined by their respective diffraction peak intensities.

Based on the results above, it can be concluded that the precipitant concentration has a great effect on the phase transition of powders obtained through either reverse striking coprecipitation method or mixed precipitation method. And the effect is more remarkable when changing the precipitant concentrations for precipitating yttrium ions.

When the precipitant concentration applied for precipitating yttrium ions is 1.5 M, precursors obtained cannot convert into YAG phase completely even after being calcined at 1350 °C, and transient phases seem to be reluctant to react with each other to convert into YAG phase. Especially for YAM phase, it begins to appear at 900 °C, and still exists even after precursors being calcined at 1350 °C. When the precipitant concentration applied for precipitating yttrium ions is 0.5 M, it is quite easy for precursors to convert into YAG phase completely and the calcining temperature needed is much lower. Either YAM phase is not detected obviously or it converts into YAP phase then into the final YAG phase at lower temperatures (≤1200 °C). And YAM phase cannot be detected in the powders obtained at 1050 °C any more.

When changing the precipitant concentrations for precipitating aluminum ions, it can be concluded that the lower precipitant concentration can decrease the phase formation temperature of YAG phase by comparing the phase transition procedure of precursor M2 and M3. For precursor M2, it can convert into YAG phase completely after being calcined at 1200 °C. While for precursor M3, it can convert into YAG phase after being calcined at 1050 °C which is 150 °C lower than M2.

3.2. Morphologies of YAG precursors and corresponding powders obtained at 750 °C

Fig. 4 shows the morphologies of precursor C1 and C2 and calcined powder CC1 and CC2 obtained at 750 °C. As seen in the figure, nearly spherical particles of nanoscale can be observed in the precursor C1. While for C2, particles of two kinds of quite different morphologies can be observed, one is cluster of particles nearly spherical in shape and the other is flake-like particle with the size of micron level. After being calcined at 750 °C, the size of flake-like particles is decreased but still of micron level.

Fig. 5 shows the morphologies of precursor M1–M3 and calcined powder MC1–MC3 obtained at 750 °C. As shown in the figure, two kinds of different morphologies can be observed in M1 and MC1, and the difference between M1 and MC1 is the size of flake-shaped particles. That is similar with the case of C2. Particles with two kinds of different morphologies can be observed in M2, but the size of flake-shaped particles is much smaller and of hundreds of nanometers level. After being calcined, the flake-shaped particles disappear. There are still two kinds of different morphologies in the powder MC2, one is clusters of smaller particles and the other is better dispersed spherical particles. The morphologies of M3 and MC3 are very alike, and only spherical particles of about 100 nm can be observed.

3.3. Characteristics of yttria and alumina powders prepared using different methods and under different precipitant concentrations

In order to investigate the effect mechanism of precipitant concentration, the properties of alumina and yttria powders prepared under different precipitant concentrations and using different precipitation method were studied. Fig. 6 shows the XRD patterns of Y1, Y2 and Y3. As shown in Fig. 6, the precursor Y1 is determined as hydrated yttrium carbonate. For

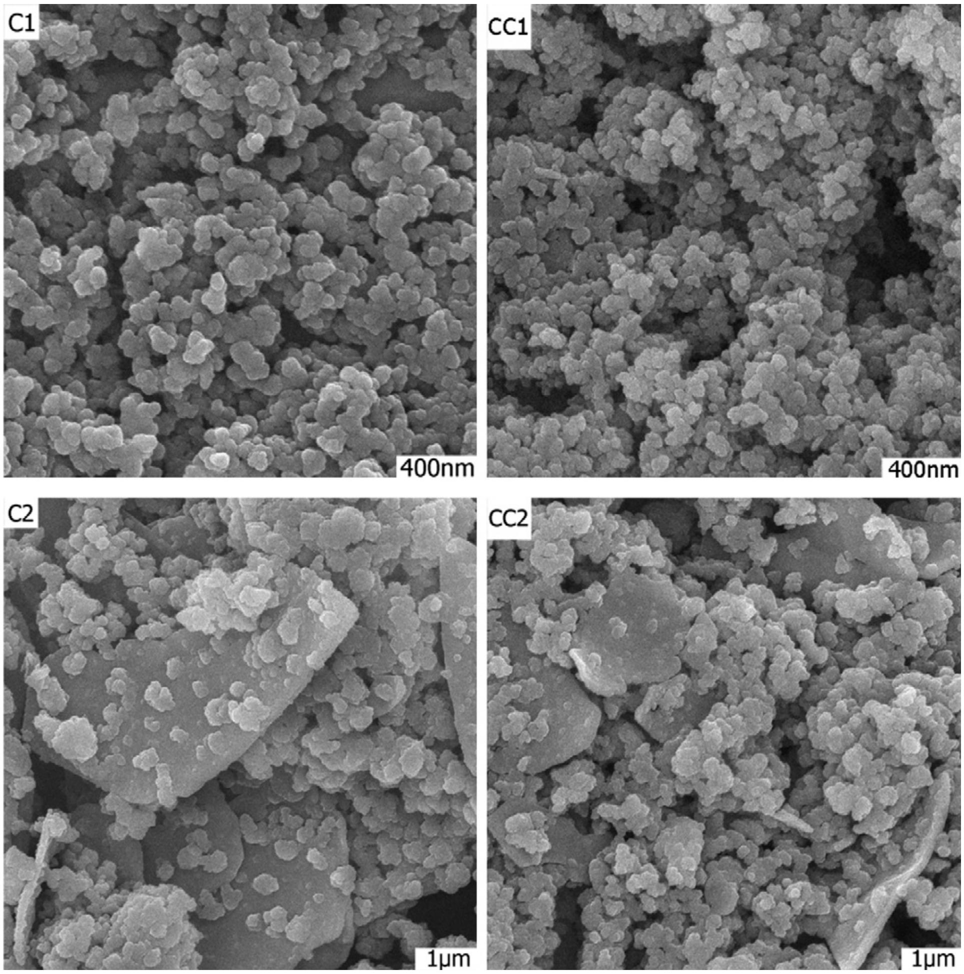

Fig. 4. The morphologies of C1, C2, CC1 and CC2.

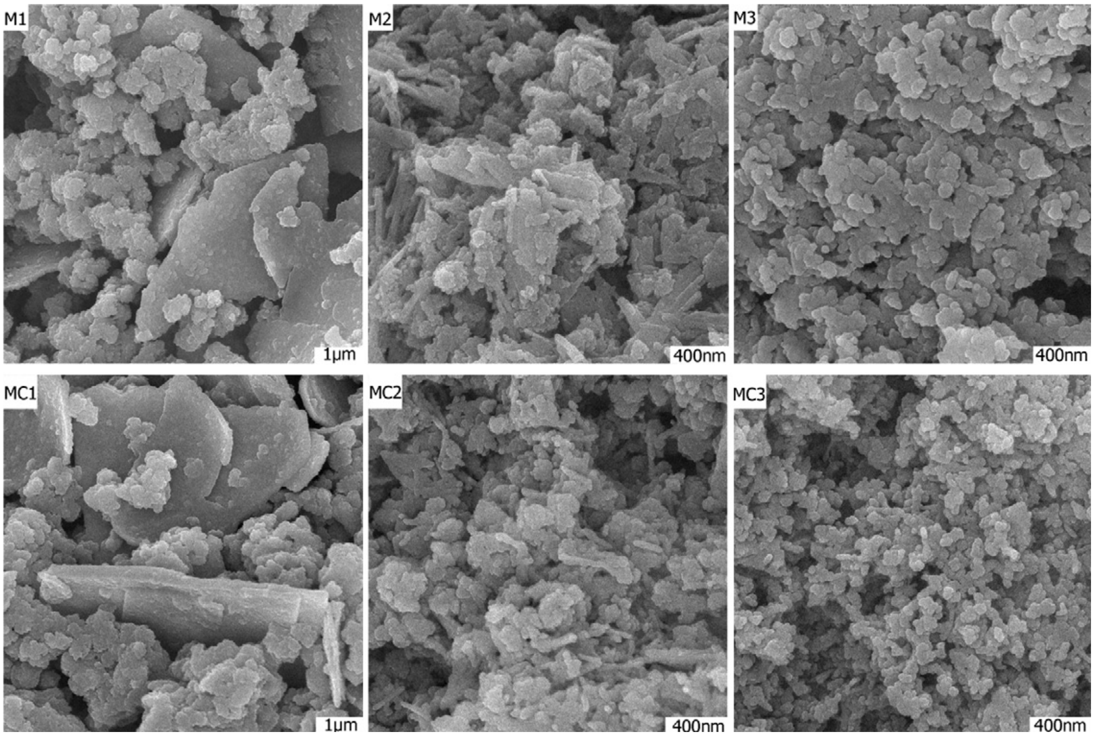

Fig. 5. The morphologies of M1–M3 and MC1–MC3.

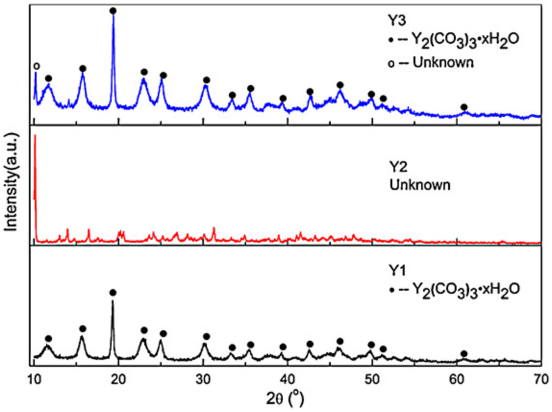

Fig. 6. The X-ray diffraction analysis of precursor Y1–Y3.

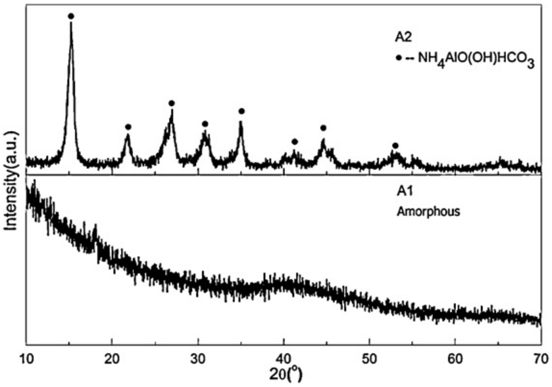

Fig. 8. The X-ray diffraction analysis of precursor A1 and A2.

Y2, the phase cannot be determined although many obvious diffraction peaks are detected, and a striking strong diffraction peak around 10° can be observed. While for Y3, most diffraction peaks correspond to hydrated yttrium carbonate, and one peak similar with the strongest one in the case of Y2 can also be detected.

The morphologies of Y1–Y3 and YC1–YC3 are shown in Fig. 7. And the yttria powders were obtained by calcining the precursors at 750 °C for 2 h. As shown in Fig. 7, small flake-shaped particles can be seen in the precursor Y1, and part of the particles seems to be formed by the aggregation of spherical particles of smaller than 100 nm. After being calcined, only spherical particles of about 100 nm can be observed. The rhombohedral flake-shaped particle can be seen in the Y2 precursor. The particle size is larger than 10 μm in plane directions and about 500 nm in thickness direction. And the flake-shaped particles tend to stack together. The morphology of the powder YC2 is similar with its precursor, and the remarkable difference is the particle size. The precursor Y3 is also small flake-shaped particle, but the flake shape seems more perfect compared with Y1. Particles with two different kinds of morphologies can be observed in the powder YC3, one is large flake-shaped particle and about 100 nm thick, the other is rod-like particles formed by the aggregation of small particles.

The XRD analysis of precursor A1 and A2 is shown in Fig. 8. It is confirmed that the precursor A1 is amorphous and A2 is ammonium aluminum carbonate hydroxide.

Fig. 9 shows the morphologies of A1, A2, AC1 and AC2. As seen in the figure, the particle size of precursor A1 is about 50–100 nm, and particles aggregate to some extent. While for A2,

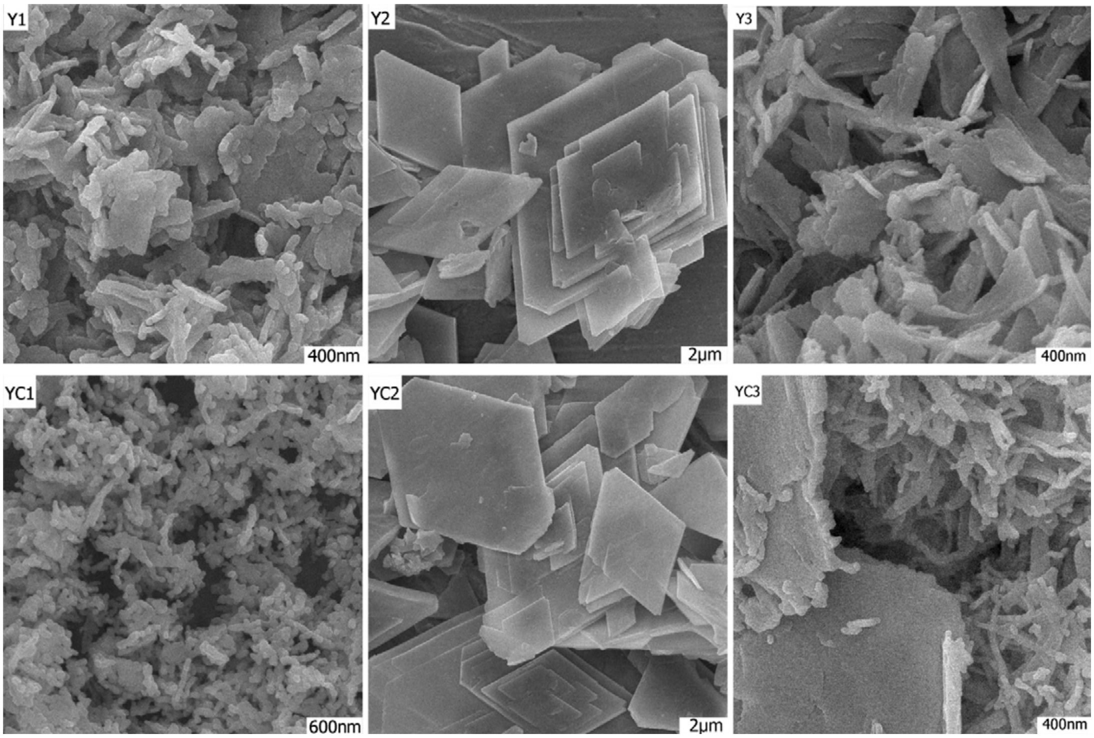

Fig. 7. The morphologies of Y1–Y3 and YC1–YC3.

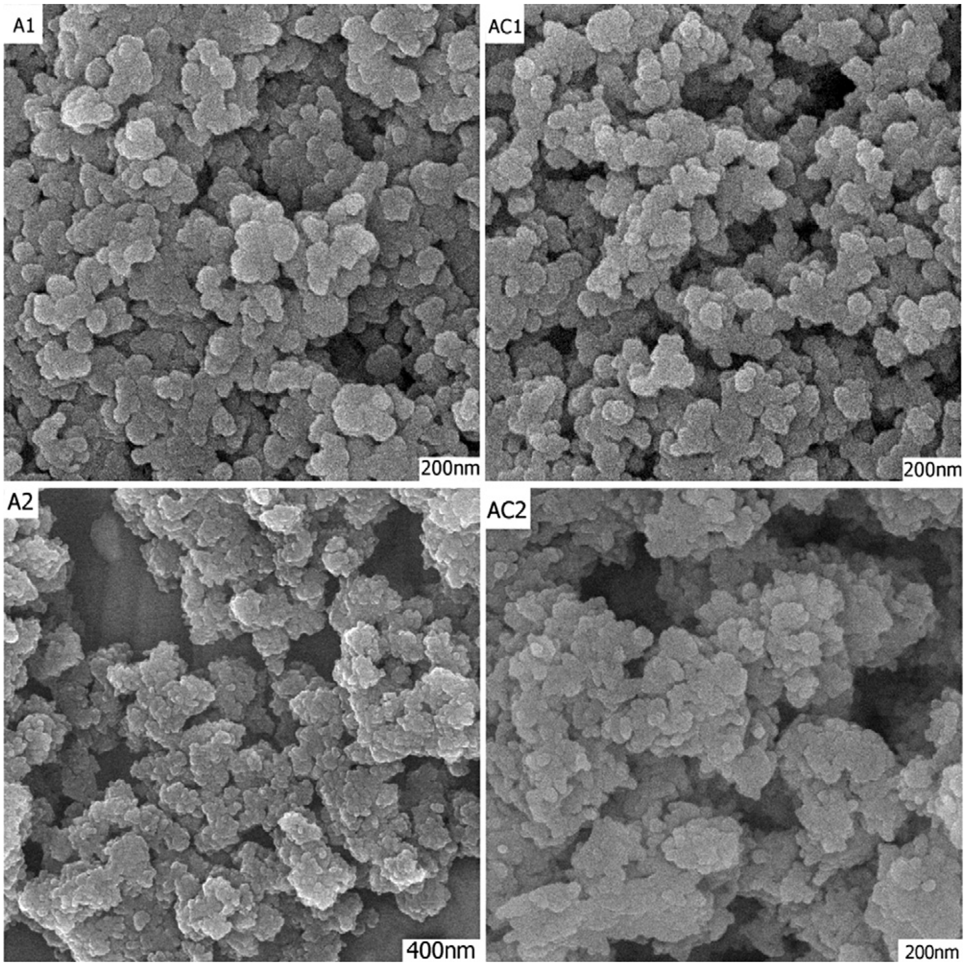

Fig. 9. The morphologies of A1, A2, AC1 and AC2.

the primary particle is smaller than 50 nm, but the particles aggregate into clusters of several hundred nanometers. The morphologies of the powder AC1 and AC2 are quite similar with their corresponding precursors.

3.4. Discussion

The phase transition procedure of precursors to YAG powders is actually a solid-state reaction between alumina and yttria powders. Based on the results in Figs. 2 and 3, the precursors, which are actually mixtures of aluminum precipitate and yttrium precipitate, convert into mixtures of alumina and yttria powders after being calcined at low temperature. The alumina diffraction peaks are not observed obviously because the alumina powder obtained at low temperature is in the form of metastable phases such as γ-Al_2O_3 and θ-Al_2O_3, and the diffraction intensity of those phases is so weak that the peaks are concealed [13].

As known to us, diffusion of ions plays an important role in solid-state reactions. It has been revealed in the precious works [14,15] that the reaction of aluminum and yttrium oxides is processed by the diffusion of aluminum ions into the yttrium oxides mainly, and the size of yttria particle determines the diffusion distance. The diffusion distance is also affected by the homogeneity of mixtures and the decrease in homogeneity will result in the increase of the phase formation temperature [16].

As discussed before, the phase transition procedures of precursor C2 and M1, during the preparation processes of which the precipitant concentrations applied for precipitating yttrium ions are both 1.5 M, are quite similar. Powder CC2 and MC1 were obtained by calcining precursor C2 and M1 at 750 °C. As shown in Figs. 4 and 5, the large flake-shaped particles of several micrometers can be observed in the powders CC2 and MC1. It can be judged that the flake-shaped particles are yttria particles based on the results in Fig. 7. The size of yttria particles is so large that the diffusion distance is lengthened during the process of reaction between alumina and yttria. Further more, the oversize of yttria particles decreases the homogeneity of oxide mixtures, and makes the diffusion of aluminum ions into yttria particles more difficult. So the ratio of yttrium and aluminum interior the yttria particles is higher than stoichiometric ratio of YAG phase. That will result in the formation of intermediate phases which are poor in aluminum content and make it difficult for the intermediate phases to convert into YAG phase. Therefore, as summarized in Table 2, it is very difficult for precursor C2 and M1 to convert into YAG phase completely, and the intermediate phases can still be detected even after the precursors are calcined at higher temperatures (≥1200 °C). For YAP, it forms at about 1050 °C, and cannot be detected any more at 1350 °C. While for YAM, it forms at lower temperature (about 900 °C), and can still be detected even after calcining at 1350 °C. And a little amount of alumina converts into the form of α-Al_2O_3 phase before it diffuses into the interior of yttria particles to form compounds at high temperature (about 1200 °C). Temperature higher than 1350 °C is essential for the preparation of powders of single YAG phase.

Precursor C1, M2 and M3, during the preparation processes of which the precipitant concentrations applied for precipitating yttrium ions are both 0.5 M, can convert into YAG phase completely at lower temperatures (≤1200 °C). Powder CC1, MC2 and MC3 were obtained by calcining corresponding precursors at 750 °C. As also shown in Figs. 4 and 5, only spherical particles can be observed in the powder CC1 and CC3. Although flake-shaped particles can be observed in the powder YC3, the similar phenomenon is not observed in the powder CC1. That might be resulted from the mutual effect of alumina precipitate and yttria precipitate during the process of coprecipitation. While in the powder MC2, the clusters observed are determined as alumina according to the results in Fig. 9, and the better dispersed particles are yttria particles. It can be concluded that the particle size of yttria powder is very small and the diffusion distance of aluminum ions into the yttria particles is very short, so it is very easy for the intermediate phases to convert into the target phase YAG. Therefore, as summarized in Table 2, intermediate phases can only be detected in the powders obtained at lower temperatures (≤1050 °C) during the phase transition process of precursor C1, M2 and M3, and powders of single YAG phase can be obtained at lower temperatures (≤1200 °C).

It can be concluded that lower precipitant concentration is preferable to the formation of YAG phase from the perspective of precipitating yttrium ions. Because under higher precipitant concentration, the yttria particles obtained is flake-shaped and of micron level, while under lower precipitant concentration, the yttria particles obtained is spherical and smaller than 100 nm. The oversize of yttria particles can result in the decrease of homogeneity of oxide mixture obtained at low temperature and the increase of ions diffusion distance, therefore the temperature for preparation of YAG powder is elevated.

Compare precursor M2 and M3, during the preparation process of which the precipitant concentrations applied for precipitating yttrium ions are both 0.5 M, but the concentrations applied for precipitating aluminum ions are different, 1.5 M for M2 and 0.5 M for M3, the phase formation temperatures of YAG are different, 1200 °C for M2 and 1050 °C for M3. As shown in Fig. 5, clusters of several hundred nanometers can be seen clearly in the powder MC2. While in the powder MC3, no similar phenomenon can be observed. As mentioned above, the clusters are alumina powders. And clusters will result in the decrease in homogeneity and increase the diffusion distance of aluminum ions into yttria particles. So the essential temperature for the formation of YAG phase is increased. That is why the YAG formation temperatures of M2 and M3 are different. The clusters are very big, but still much smaller than micron scale, so the intermediate phases can easily convert into YAG phase at lower temperatures (≤1200 °C).

It can be concluded that the low precipitant concentration is preferable to the formation of YAG phase because of the formation of alumina clusters from the perspective of precipitating aluminum ions. The formation of alumina clusters can reduce the homogeneity of oxide mixture and increase the temperature essential for the preparation of YAG powder. The formation of alumina clusters can be explained according to the theory of crystal nucleation and growth [17]. Higher precipitant concentration will result in larger supersaturation in local area during the process of precipitating reaction. Higher nucleation rate and smaller critical nucleus size will be caused successively, and nucleuses tend to aggregate to from clusters easily because of much higher surface energy and higher nucleus concentration. While under the condition of lower precipitant concentration, the nucleation rate is much lower and critical nucleus size is bigger due to the lower supersaturation, the tendency of aggregation of nucleuses is mitigated greatly by the decrease of surface energy and nucleus concentration. Therefore better dispersed powder can be obtained.

4. Conclusions

In this paper, the effect of precipitant concentration on the formation procedure of YAG phase which is actually a solid reaction controlled by the diffusion of aluminum ions into the yttria particles is investigated and the precipitant used is ammonium bicarbonate. It is found that higher precipitant concentration (1.5 M) is not preferable to the formation of YAG phase, and the intermediate phases have not converted into the final YAG phase completely when the calcining temperature reaches 1350 °C. While lower precipitant concentration (0.5 M) is favorable to the phase transition procedures. And intermediate phases can convert into YAG phase at the temperature of 1050 °C. Under higher precipitant concentration, the size of yttria particles formed is in micron level and alumina particle is in the form of clusters which are formed by the aggregation of smaller nucleuses, and the powder homogeneity is relatively poor, so the element diffusion distance is lengthened and higher temperature (≥1350 °C) is essential for the completion of phase transitions. Under lower precipitant concentration, the sizes of yttria particles and alumina particles are both smaller than 100 nm and the powder homogeneity is improved, so the phase transition procedure can complete at lower temperatures (≤1200 °C).

Acknowledgements

This work was supported by the Project 863 (no. 2010AA0301587003), the Major Basic Research Program of Natural Science Foundation of China (no. 50990303), the Project for Young Scientists Fund of National Natural Science Foundation of China (no. 51002172) and Key Program of Shanghai Association of Science and Technology (no. 10JC1416000).

References

[1] A. Ikesue, Y.L. Aung, T. Taira, T. Kamimura, K. Yoshida, G.L. Messing, Progress in ceramic lasers, Annu. Rev. Mater. Res. 36 (2006) 397–429.

[2] R.C. Pullar, M.D. Taylor, A.K. Bhattacharya, The sintering behaviour, mechanical properties and creep resistance of aligned polycrystalline yttrium aluminium garnet (YAG) fibres, produced from an aqueous sol–gel precursor, J. Eur. Ceram. Soc. 19 (9) (1999) 1747–1758.

[3] S. Karato, Z. Wang, K. Fujino, High-temperature creep of yttrium–aluminum–garnet single-crystals, J. Mater. Sci. 29 (24) (1994) 6458–6462.

[4] A. Ikesue, T. Kinoshita, K. Kamata, K. Yoshida, Fabrication, Optical-properties of high-performance polycrystalline Nd–YAG ceramics for solid-state lasers, J. Am. Ceram. Soc. 78 (4) (1995) 1033–1040.

[5] Y.S. Wu, J. Li, Y.B. Pan, J.K. Guo, B.X. Jiang, Y. Xu, J. Xu, Diode-pumped Yb:YAG ceramic laser, J. Am. Ceram. Soc. 90 (10) (2007) 3334–3337.

[6] Y. Shi, Y.B. Pan, X.Q. Feng, J. Li, J.K. Guo, Fabrication and luminescence study of Ce(3+)-doped YAG transparent ceramics, J. Inorg. Mater. 25 (2) (2010) 125–128.

[7] T. Yanagitani, H. Yagi, M. Ichikawa, Production of yttrium–aluminum–garnet fine powder, JP Patent 10-101333.

[8] T. Yanagitani, H. Yagi, Y. Hiro, Production of fine powder of yttrium aluminum garnet, JP Patent 10-101411.

[9] J.G. Li, J.H. Lee, T. Mori, Y. Yajima, S. Takenouchi, T. Ikegami, Crystal phase and sinterability of wet-chemically derived YAG powders, J. Ceram. Soc. Jpn. 108 (5) (2000) 439–444.

[10] P. Palmero, C. Esnouf, L. Montanaro, G. Fantozzi, Influence of the co-precipitation temperature on phase evolution in yttrium–aluminum oxide materials, J. Eur. Ceram. Soc. 25 (9) (2005) 1565–1573.

[11] X.X. Li, W.J. Wang, Preparation of uniformly dispersed YAG ultrafine powders by co-precipitation method with SDS treatment, Powder Technol. 196 (1) (2009) 26–29.

[12] H. Gong, D.Y. Tang, H. Huang, J. Ma, Agglomeration control of Nd:YAG nanoparticles via freeze drying for transparent Nd:YAG ceramics, J. Am. Ceram. Soc. 92 (4) (2009) 812–817.

[13] K. Morinaga, T. Torikai, K. Nakagawa, S. Fujino, Fabrication of fine alpha-alumina powders by thermal decomposition of ammonium aluminum carbonate hydroxide (AACH), Acta Mater. 48 (18–19) (2000) 4735–4741.

[14] A.Y. Neiman, E.V. Tkachenko, L.A. Kvichko, L.A. Kotok, Conditions macromechanism of solid-phase synthesis of yttrium aluminates, Russ. J. Inorg. Chem. 25 (9) (1980) 2340–2345.

[15] V.B. Glushkova, V.A. Krzhizhanovskaya, O.N. Egorova, Y.P. Udalov, L.P. Kachalova, Interaction of yttrium and aluminum-oxides, Inorg. Mater. 19 (1) (1983) 80–84.

[16] F. Ivanauskas, A. Kareiva, B. Lapcun, On the modeling of solid state reactions. synthesis of YAG, J. Mater. Chem. 37 (4) (2005) 365–376.

[17] D. Feng, C.X. Shi, Z.G. Liu, Introduction of Materials Science, 1st ed., Chemical Industry Press, Beijing, 2002.